

## The influence of variation in track level and support system stiffness over longer lengths of track for track performance and vehicle track interaction

David Milne, John Harkness, Louis Le Pen & William Powrie

To cite this article: David Milne, John Harkness, Louis Le Pen & William Powrie (2019): The influence of variation in track level and support system stiffness over longer lengths of track for track performance and vehicle track interaction, Vehicle System Dynamics, DOI: [10.1080/00423114.2019.1677920](https://doi.org/10.1080/00423114.2019.1677920)

To link to this article: <https://doi.org/10.1080/00423114.2019.1677920>



© 2019 The Author(s). Published by Informa UK Limited, trading as Taylor & Francis Group



Published online: 13 Oct 2019.



Submit your article to this journal [↗](#)



Article views: 669



View related articles [↗](#)



View Crossmark data [↗](#)

# The influence of variation in track level and support system stiffness over longer lengths of track for track performance and vehicle track interaction

David Milne , John Harkness , Louis Le Pen  and William Powrie 

School of Engineering, University of Southampton, Southampton, UK

## ABSTRACT

Differential settlement and development of track geometry irregularity drives the need for maintenance of ballasted railway tracks. Predicting this requires an understanding of how train loading and the resulting stresses vary and are distributed along the track and how the track responds. Irregularities, from differences in the unloaded level and deflection under load (from variation in stiffness and load) influence the wheel-rail contact force along the track. The stiffness will also influence the distribution of stress into the ground. To investigate variation in the (unloaded) track level and support system stiffness along a railway, stiffness, track deflection and sleeper level surveys were carried out along a 200 m length of track. Measurements were taken at every sleeper using total station for track level and accelerometers to calculate deflection, together with a frequency-based analysis for the track support system stiffness. A simple 2D vehicle track interaction model was used to study the influence of the unloaded sleeper level, the variation in track stiffness and any identified voiding for the performance of the track. Here, the unloaded level was more significant for the loaded level and the wheel / rail contact forces than the variation in track stiffness, which was most importance for the deflections under load.

## ARTICLE HISTORY

Received 24 January 2019  
Revised 2 September 2019  
Accepted 30 September 2019

## KEYWORDS

Track stiffness; track level; vehicle-track interaction; stiffness measurement; rail surveying; track vibration

## Introduction

An ambition of the rail industry in the UK and elsewhere is to use ever-advancing monitoring and modelling techniques to manage the performance of railway track and inform maintenance planning as part of a strategy to improve reliability, increase capacity, reduce delays, enhance safety and drive down costs [1]. This might include forecasting attributes of the physical behaviour of the track, such as track deflection and changes in track level through differential settlement as functions of train loading, along an entire route to better understand maintenance needs. For such an approach to be effective, it is necessary to understand which aspects of the physical properties of railway track are significant, and should be measured, for simulating relevant aspects of behaviour in a computationally efficient way.

**CONTACT** David Milne  d.milne@soton.ac.uk

© 2019 The Author(s). Published by Informa UK Limited, trading as Taylor & Francis Group

This is an Open Access article distributed under the terms of the Creative Commons Attribution License (<http://creativecommons.org/licenses/by/4.0/>), which permits unrestricted use, distribution, and reproduction in any medium, provided the original work is properly cited.

Significant deviations or high variability in the loaded track level will necessitate maintenance [2]. To understand and predict the development of differential settlement, it is necessary to understand how train loads and resulting stresses are distributed into the trackbed and subgrade and how they vary along a track length. These will be influenced by variations in both track stiffness and unloaded track geometry (level), which are likely to change over the life of a track owing to the development of differential settlement and maintenance.

The track geometry is known to control the vehicle / track interaction forces [3,4]. Vehicle / track interaction modelling can be used to understand the role of the track level and the track support stiffness. Multi-body simulation is routinely carried out using software such as Vampire [5], NUCARS [6] and VI-Rail [7]. These programmes simulate the dynamic response of a vehicle to measured loaded track geometry (which implicitly includes the effect of any variation in track support stiffness), but generally assume a uniform track support stiffness or possibly rigid track in a simplified model [8]. These types of model can calculate wheel / rail contact forces but do not attempt to replicate the full behaviour of the track; for this purpose, the finite element method, with its ability to model more comprehensively the vehicle and track together, is generally used [9–17]. Finite element analysis enables variations in track stiffness and rail irregularities to be modelled but is far more computationally intensive, so is not routinely implemented for long lengths of track.

Track stiffness is known to be an important parameter influencing the performance of railway track [18,19]. Support conditions have been shown to vary from sleeper to sleeper [20–24] and over longer lengths of track [25,26]. Changes in support stiffness will affect vehicle / track interaction and track deflection [27–29] and are often associated with deterioration and increased maintenance need [30–32]. This is because a differential stiffness will cause an uneven track level under load, influence how the stresses induced by train loading are distributed beneath the track [33–35], and govern how much energy is dissipated into the track [36].

The objective of this research was to assess the significance of real variations in track support system stiffness, unloaded track level (geometry) and non-linearity due to voiding on the modelled behaviour of a long length of track, through simulations using data obtained from large scale trackside measurements. Few if any previous studies have separated the roles of the track level and the support conditions over long lengths of track in simulations using input parameters based on real data of both. This study seeks to identify which parameters are important for reproducing realistic vehicle and track behaviour and interactions between the two, while challenging the assumptions made to obtain those parameters, with a view to forecasting performance over long lengths of track – possibly using simpler models.

## Background

To investigate the influence of variation in track level and track stiffness over an extended length of track, measurements of track level, track stiffness and track deflection were required. In this study, the track support system stiffness is quantified by the track support system modulus  $k$ , defined as the support force  $q$  per unit length of rail, per unit

displacement  $w$ :

$$k = \frac{q}{w} \quad (1)$$

The track support system modulus is a global measure of the support seen at the rail. For analytical convenience, it is often assumed to be constant – at least to a first order approximation – but in reality will vary along the track. The track support system modulus combines the effects of all the resilient elements below the rail (rail pads, ballast, sub ballast, the foundation and possibly under sleeper or pads and mats).

Lineside measurement techniques can be used to investigate track performance by monitoring the trackbed or sleeper deflections and determining track stiffness. A variety of technologies could be used for this, including high speed video recording of track-mounted targets for digital image correlation, deflectometers anchored at depth, position sensitive devices, lasers and inertial sensors such as geophones or accelerometers [20–24,37]. Track stiffness can be obtained from these types of measurements based on the load-deflection behaviour of the track [38–41], or by analysing the spectrum of low frequency vibrations without the need to know the load [42,43]. Absolute sleeper levels can be measured from the side of the track by conventional surveying.

Most lineside monitoring techniques produce discrete measurements and normally require one sensor per measurement point for each measurand. The cost of equipment and potential volume of data have tended to limit the extent of previous deployments to a few sleepers (tens of metres), so most studies have tended to focus on a specific feature e.g. a transition [22,23,44–46] or poor ground conditions [20,41]. Lower cost transducers and data acquisition systems, e.g. MEMS sensors and microprocessors, mean that larger scale deployments are increasingly possible.

Track level and stiffness variation have recently been investigated using rolling measurements [47]. Although rolling measurements might be necessary for a route level study, the research reported in this paper used established, high-surety lineside monitoring and surveying techniques to measure the level, dynamic deflection and stiffness of the track to guarantee a spatial resolution at the sleeper spacing level and the clear decoupling of unloaded track levels from deflections under load. The measurements were then used to parameterise and assess simulations from a 2D dynamic finite element vehicle track interaction model.

## Methods

### *Site description*

The site studied covered a  $\sim 200$  m length (about 350 sleepers) of track on a ballasted high-speed railway. It was selected as representative of normal, straight, high speed plain line track. The infrastructure manager advised that the first 200 sleepers at the site have historically needed more maintenance than the remainder. The track comprised CEN 60 E1 rails on railpads, supported by twin block sleepers at 0.6 m spacing. The railpads were found to have a static stiffness of 84 MN/m in laboratory tests. The track has a uniform downward gradient of 1.4% in the usual direction of travel. Most of the site is in a shallow cutting. Pre-construction boreholes showed a thin layer of clayey sand overlying dense sand [48]. It is likely that the trackbed was built onto the dense sand. The site was regularly

trafficked by three types of train: the Class 395 Javelin, the Class 373 Eurostar and the Class 374 Velaro. The survey and the lineside instrumentation were focused on one running rail, at the edge (cess side) of the track.

### **Survey**

The sleeper level survey was carried out using a Trimble S9 self-levelling, automatic-tracking total station and active prism (Figure 1). The prism was placed in line with the manufacturer's markings on a sleeper, and the total station was used to track and record the co-ordinates and height of the prism as it was moved sequentially from sleeper to sleeper along the track. The total station had an angular accuracy of  $0.5''$ , and was the best commercially available at the time.

### **Deflection and stiffness survey**

The deflection and stiffness survey was carried out using Gulf Coast Data Concepts X16 micro-electro-mechanical-systems (MEMS) accelerometers. These are stand-alone devices, each containing an ADXL 345 digital MEMS accelerometer, a microcontroller programmed as a data acquisition unit, a real time clock, a memory card and a battery. They were validated using a procedure similar to that described in [49]. About 80 of these devices were placed on successive sleeper ends, primarily on the outside of the track, and were moved along the site during consecutive night-time possessions. This was done in two batches of 200 sleepers, with an overlap of 50 sleeper ends, approximately 3 months apart. Results were combined to give a dataset for a 200 m section of track Figure 2.

The devices were programmed to record continuously at 400 Hz. After deployment, the devices were recovered and the data downloaded. An acceleration threshold was used to identify passing trains and the data were sorted by train type. The sampled accelerations



**Figure 1.** Total station and active prism.



**Figure 2.** Stand-alone MEMS accelerometer used for deflection and stiffness survey deployed on a sleeper end.

were filtered and integrated twice to obtain displacements, using 4th order high- and low-pass Butterworth filters with cut on and cut off frequencies of 2 and 40 Hz respectively [37]. This covers the frequency range of interest for the major trackbed motions at the site [43]. Example sleeper deflection data and the corresponding frequency spectrum from the site studied are shown in Figure 3.

To facilitate comparison of performance at multiple locations, a statistical process was used to characterise the range of downward sleeper deflections for each train passage. This uses the cumulative distribution function for track deflection to identify the at-rest position and downward movement [50]. The track support system modulus was obtained by

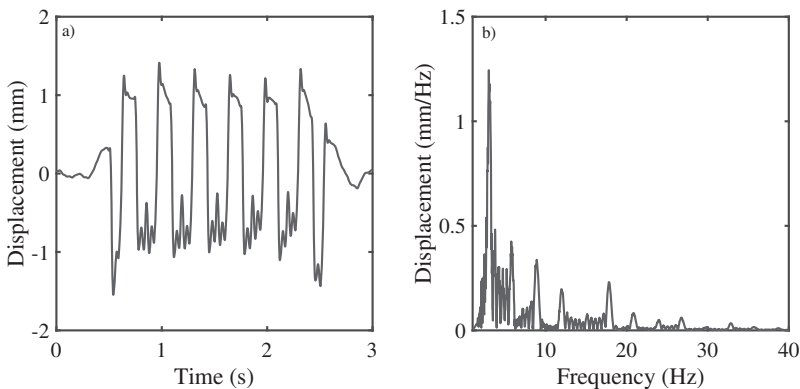


**Figure 3.** Example deflection data obtained from a MEMS accelerometer at the study site.



analysing the Fourier spectrum for sleeper acceleration, as outlined below for analysing the measured and simulated sleeper vibrations.

Equation 1 is a general definition of the track support system modulus, which in reality must be expected to vary along the track. Practically, it is challenging to take all the measurements needed to evaluate this variation; hence for analytical convenience, it is often assumed to take a constant, representative value. A common simple model for track deflection is a continuous beam on an elastic foundation, which for uniform support conditions has a closed form solution. The governing equation in this case is [40,51]:

$$EI \frac{d^4 w(x)}{dx^4} + kw(x) = P(x) \quad (2)$$

where (in addition to the terms already defined)  $EI$  is the bending stiffness of the rail,  $x$  is the distance along the rail and  $P$  is a function representing the loading on the track. The closed form solution can be used as a basis for interpretation of measured or simulated low frequency track vibration in the time or frequency domain [e.g. 39,43].

Track vibration spectra for trains that comprise multiple near identical vehicles, e.g. the Javelin in Figure 3(b), contain peaks at integer multiples of the vehicle passing frequency (i.e. the train speed divided by the primary vehicle length), although certain peaks are suppressed. The frequency and magnitude of these dominant spectral peaks can be shown to depend primarily on the train geometry and the track stiffness [42,43,52,53]. The ratio of the magnitudes of two of these peaks can be related to the track support system modulus, without needing to know the load. Certain pairs of peaks are preferable for reasons including the train geometry and transducer noise [43].

Using the Fourier transform,  $W$ , of the closed form solution of the quasi-static form of Equation 2 assuming uniform support, it can be shown [42] that the expected magnitude ratio for two peaks at multiples of the vehicle passing frequency is given by:

$$\frac{W(af_1)}{W(bf_1)} = \frac{L_v^4 k + 16EIb^4 \pi^4 \sum_{n=1}^N e^{-\frac{i2\pi ax_n}{L_v}}}{L_v^4 k + 16EIa^4 \pi^4 \sum_{n=1}^N e^{-\frac{i2\pi bx_n}{L_v}}} \quad (3)$$

where  $a$  and  $b$  are integer multiples of the vehicle passing frequency  $f_1$ ,  $L_v$  is the length of the primary vehicle, and  $x_n$  is the distance between the first and  $n^{\text{th}}$  wheel of the train. This ratio is independent of the load.

The relationship between the support system modulus and the magnitude ratio of selected displacement peaks for the trains passing the site is shown in Figure 4. The corresponding curves for velocity or acceleration data can be found by multiplying (once or twice, respectively) by the ratio of the frequencies chosen. The ratio of the 3<sup>rd</sup> and 7<sup>th</sup> multiples of the vehicle passing frequency was used for the Javelin and the Velaro, and the ratio of the 2<sup>nd</sup> and 6<sup>th</sup> multiples for the Eurostar.

Equation 2, which was used for interpreting the measurements, is a simplification for real track. It is based on quasi-static loading, and linear and uniform track support conditions. This means that non-uniformity, non-linearity or inertial effects may affect the results of this analysis, possibly in a non-systematic way. Nonetheless, the model does capture the fundamental behaviour of the track and provides a simple and effective method for obtaining a measure of the track support system stiffness without knowing the load. The method facilitates efficient analysis of the large volumes of vibration data needed

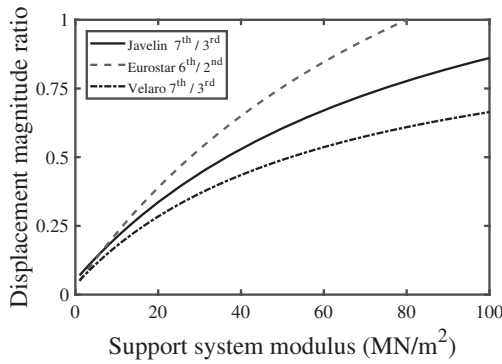


**Figure 4.** Relationship between the ratio of magnitudes of pairs of dominant train load frequencies for different trains used to obtain the track support system modulus in this study.

to understand the variation over a long length of track. Assuming uniform support to evaluate a point measurement is still likely to give a good estimate as long as the local variation in support system modulus is not excessive. (Where the variation is high, it is generally as result of a hanging sleeper and as such is usually obvious). Analysing the results of simulations with realistic track conditions enables evaluation of the technique in a controlled way; the assumptions made for interpreting the measurements are tested here.

### Simulation

Simulations were carried out using a two-dimensional dynamic finite element vehicle track interaction model programmed in *MATLAB* and solved in the time domain. The model is similar to others described and validated in the literature [9,11,54–57]. The track model comprised a single rail made up of Timoshenko beam elements, supported by rail pads represented by springs and dampers, on sleepers represented by discrete masses. (This discretised model is more complex than Equation 2. and a simpler model, without a foundation layer, would probably have been sufficient for this study). Each sleeper was connected through a spring and a damper to a ballast mass. Each ballast mass was connected longitudinally to the adjacent ballast masses and supported vertically by springs and dampers onto a foundation. The vehicle was modelled as masses representing the car body, bogie and wheels, linked by the primary and secondary suspension systems. Vehicle / track interaction was simulated using a linear contact spring. An irregular track profile may be introduced between the wheel and the rail, but the model does not include any short wavelength ( $< 20$  mm) roughness Figure 5.

Voids were modelled using bi-linear springs to represent possible non-linear behaviour arising from a gap between the sleeper and the ballast [58,59]. These springs had negligible stiffness (5 kN/m) relative to the train loads when unseated; once the sleeper deflection exceeded a specified gap the sleeper was considered to have seated on the ballast and the stiffness was increased. This idealised behaviour is illustrated in Figure 6.

The simulations presented in the following section were parameterised using combinations of constant and measured vertical sleeper positions and support system moduli, and



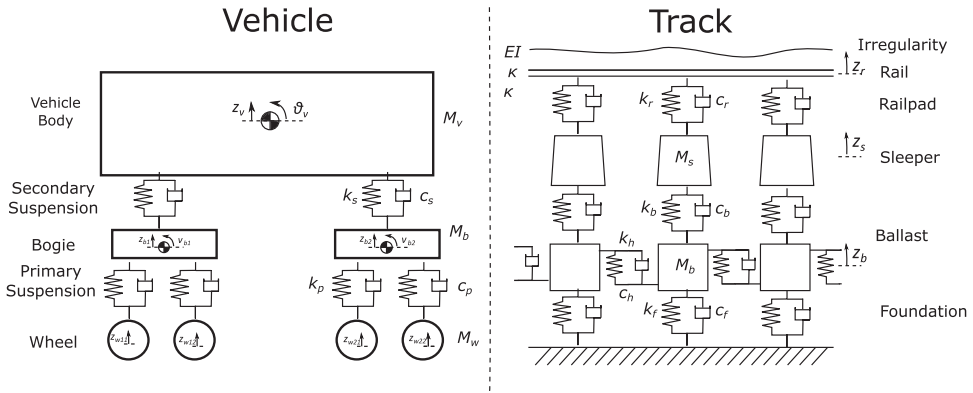


**Figure 5.** Illustration of track and vehicle model.

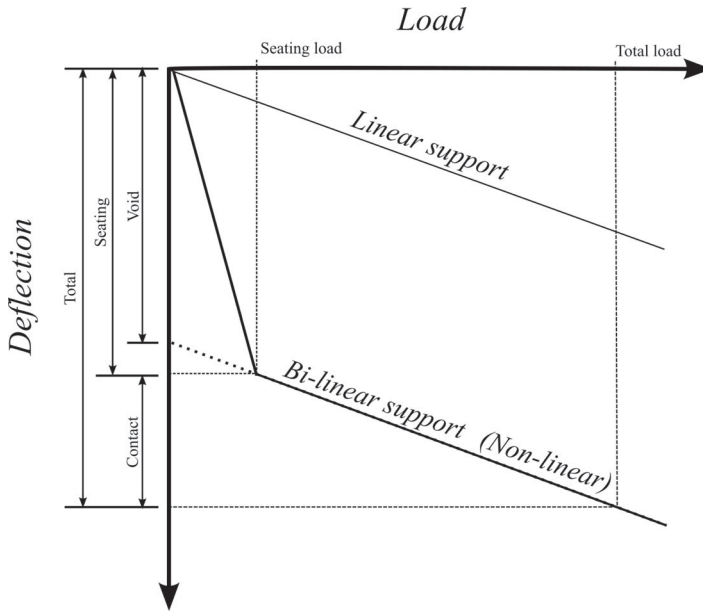


**Figure 6.** Bi-linear behaviour used to simulate voiding, after [58,59].

compared with the observed track deflections. The ballast springs were tuned so that the system stiffness matched the measurements. The masses, damping parameters and stiffnesses of the foundation and longitudinal connection were kept constant based on values obtained from the literature [54,60,61], except for the rail pad whose stiffness was determined from static laboratory testing. The foundation and the longitudinal connections were very stiff. The track parameters used are summarised in Table 1. 800 sleepers were included in the model. The central 350 were parameterised using the measured data; the 225 sleepers on each side of this zone were set level with a uniform support modulus of  $30 \text{ MN/m}^2$ , to allow the train to run evenly into and out of the zone of interest.

**Table 1.** Track parameters.

Component	Parameter	Value
Rail	Mass per length $M_r$	60 kg/m
	Bending Stiffness $El$	$6.4 \times 10^6$ Nm <sup>2</sup>
	Shear Coefficient $\kappa$	0.34
Rail Pad	Stiffness, $K_r$	$84 \times 10^6$ N/m
	Damping, $C_r$	$35 \times 10^3$ Ns/m
Sleeper mass	Mass, $M_s$	180 kg
Ballast	Mass, $M_b$	700 kg
	Stiffness, $K_b$	Tuned, otherwise $50 \times 10^6$ N/m
	Damping, $C_b$	$90 \times 10^3$ Ns/m
Longitudinal Connection	Stiffness, $K_h$	$7.84 \times 10^8$ N/m
	Damping, $C_h$	$80 \times 10^3$ Ns/m
Foundation	Stiffness, $K_f$	$7.68 \times 10^8$ N/m
	Damping, $C_f$	$65 \times 10^3$ Ns/m

The measurements gave an indication of the track support system modulus  $k$ , sampled every sleeper. The support system moduli  $k$  were converted into an equivalent discrete spring stiffness  $K$  per sleeper end at the rail by integrating over the sleeper spacing (0.6 m). Each ballast spring stiffness was then determined by assuming that the springs representing the rail pad (known), ballast (unknown) and foundation (assumed) act in series (equation 4).

$$\frac{1}{K} = \frac{1}{K_r} + \frac{1}{K_b} + \frac{1}{K_f} \quad (4)$$

For this, the longitudinal connection was neglected. In principle, this connection would have a stiffening effect on the foundation. However, as the foundation is the stiffest part of the system, the effect of the longitudinal connection on the calculated stiffness of a vertical ballast spring would be small.

Tuning the ballast springs allows the track behaviour to be simulated at system level. No attempt was made to simulate reality by assigning different stiffnesses to different layers within the subgrade, for which a far more invasive and detailed site investigation would be required.

The simulations were based on a six-vehicle train with the suspension characteristics and car body, bogie and wheel masses of the Class 395 Javelin [62], for which about half

**Table 2.** Vehicle parameters.

Component	Parameter	Value
Vehicle Geometry	Vehicle length	20.0 m
	Bogie spacing	14.2 m
	Axle spacing	2.6 m
Vehicle body	Mass, $M_v$	35600 kg
	Moment of Inertia, $I_v$	$1.07 \times 10^6$ kg.m <sup>2</sup>
Secondary Suspension	Stiffness, $K_s$	$0.605 \times 10^6$ N/m
	Damping, $C_s$	$26 \times 10^3$ Ns/m
Bogie	Mass, $M_b$	2190 kg
	Moment of Inertia, $I_b$	1460 kg.m <sup>2</sup>
Primary Suspension	Stiffness, $K_p$	$3.15 \times 10^6$ N/m
	Damping, $C_p$	$26 \times 10^3$ Ns/m
Wheel	Mass, $M_w$	765 kg

of the measurements were made. The vehicle parameters used are given in Table 2. As the model was two-dimensional and represented only one rail, the values shown in Table 1 for the vehicle body and bogie were halved for use in the simulations.

## Results and Discussion

### Measurements

Figures 7 and 8 show the results from the deflection and stiffness survey along approximately 200 m (350 sleepers) of track. Figure 7 shows the typical downward deflections (with downward taken as positive) measured at each sleeper for the three train types operating on the line studied. Figure 8 shows the results for the track support system modulus determined for each location for the three train types. These data represent the average characteristic deflection and track support system modulus for about 20 Javelins, 10 Eurostars and 10 Velaros at each sleeper.

Figures 7 and 8 show that the downward deflection and support system modulus vary along the track. In Figure 7 there are many areas where the deflections are consistently small (the typical performance of the track), but in other areas there are localised increases in deflection possibly results from low support stiffness or voiding. Figure 8 shows the variation in support system modulus along the track. Sections with lower stiffness tend to correspond to those exhibiting increased deflections. Together, these results show that the load-deflection behaviour of the track observed depended on the vehicle type.

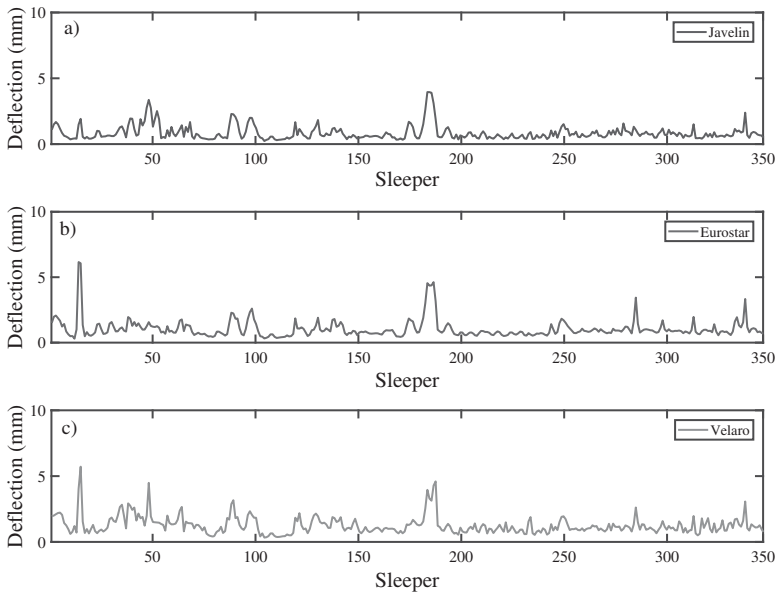


**Figure 7.** Average measured sleeper downward deflections obtained from sleeper vibration measurements along 200 m of track for (a) Javelin, (b) Eurostar and (c) Valero train types.

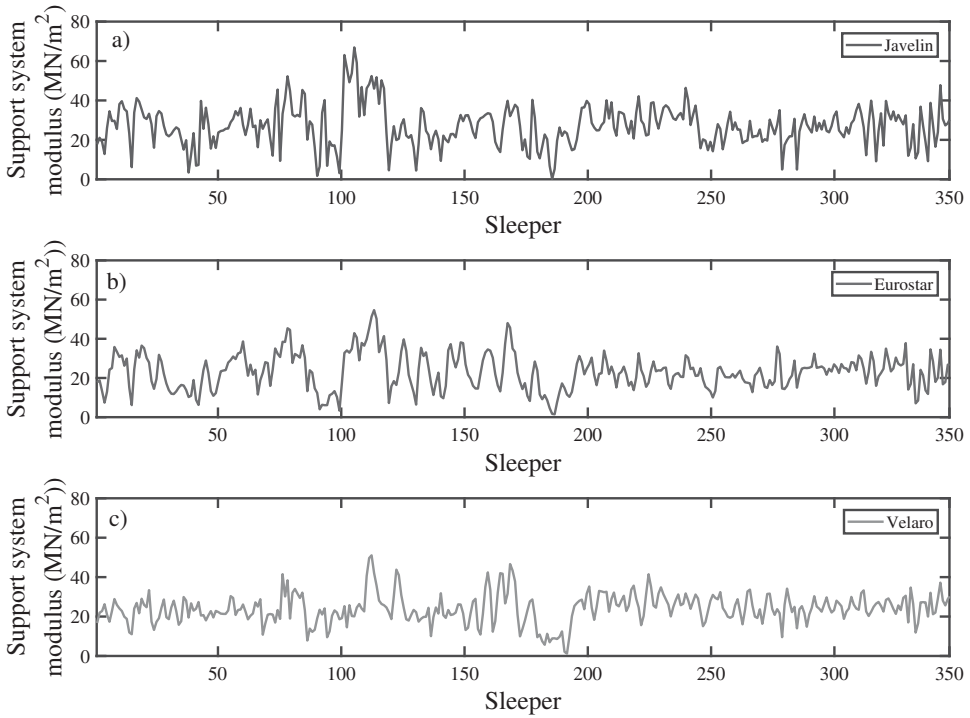


**Figure 8.** Average measured support system modulus obtained from sleeper vibration measurements along 200 m of track for (a) Javelin, (b) Eurostar and (c) Valero train types.

The data shown in Figure 8 are system values seen at the rail, and include the effect of the railpads. For the railpads present, the data shown indicate a trackbed stiffness of 70–90 MN/m per sleeper end, which is consistent with the sub 1 mm sleeper movements measured and would be considered to represent well supported track [63–66].

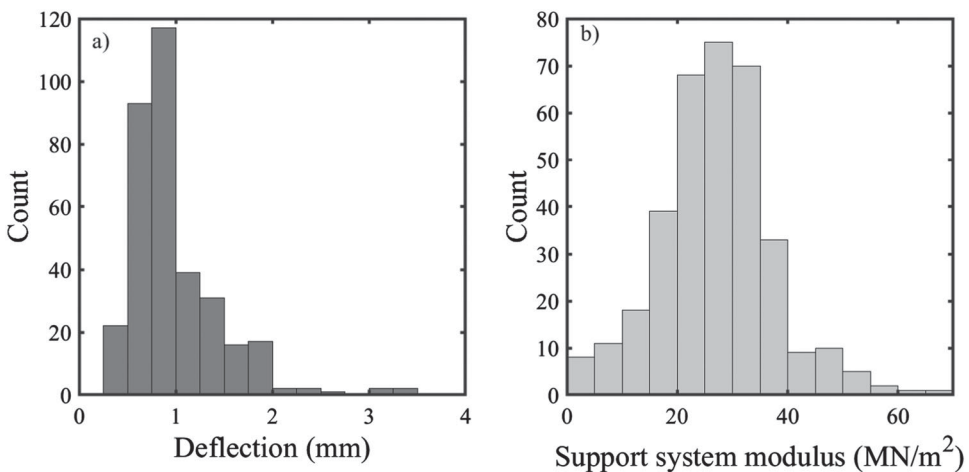


**Figure 9.** Histograms of (a.) sleeper deflection and (b) support system modulus for the Javelin data from Figure 7 and Figure 8.

Figure 9 shows histograms for sleeper deflection and support system modulus for the Javelin data from Figures 7 and 8. These data are positive valued and positive skewed, with the deflection data being more skewed than the stiffness data.

Values of mean, median, mode and standard deviation for the data in Figures 7 and 8 are shown in Table 3 for the three train types. The median or modal averages give better insight into the normal baseline performance of the trackbed, as the mean may be skewed by the larger deflections.

The patterns of variation in the deflections shown in Figure 7 are similar along the track for all three train types (the correlation coefficient between train types was more than 75% for all combinations). The amplitudes for the Eurostar and Velaro tend to be larger than those for the Javelin. This is expected as the Eurostar and the Velaro are heavier and faster than the Javelin. However, there are local differences between the shapes of the traces, particularly at sleepers with large deflections, e.g. around sleepers 15, 45–55, 85–100 and 175–185. These sleepers are likely to be poorly supported and possibly voided, leading to more complex vehicle track interaction and possibly non-linear sleeper support.

Figure 8 shows that the support system modulus varies along the track. The results differ for the three train types. Generally, the largest differences occur close to sleepers where large deflections were recorded and the support system modulus changes most abruptly: i.e. at the locations where the analysis, which assumes that any variation in support stiffness between nearby sleepers is small, is least likely to be reliable. Table 3 shows that the averages for the faster Eurostar ( $\sim 23 \text{ MN/m}^2$ ) and Velaro ( $\sim 24 \text{ MN/m}^2$ ) are less than for the Javelin ( $\sim 27 \text{ MN/m}^2$ ). This could be a consequence of analysing the results using a static model; the same effect is shown later, in the simulations.

The moduli at each sleeper were often different for each train type, leading to disagreement between results. This discrepancy may be reduced by considering data over multiple sleepers. Figure 10(a) shows the support system modulus data from Figure 8 analysed by wavelength. The spectra for the three trains are closest for wavelengths between 4 and 40 m. Figure 10(b) shows the spatial data band-pass filtered (using a 4th order Butterworth filter) for those wavelengths, with the data averaged about the mean modulus for each train. There are still differences from train to train, but lengths of track over which the modulus is high, low or more constant do coincide.

The site had a gradient of 1.4% in the direction of travel; this was removed from the data to give the relative sleeper levels, which are shown for both loaded and unloaded states in Figure 11. The loaded levels were obtained by subtracting the measured dynamic sleeper deflections to the measured sleeper level. The differences between the relative unloaded and loaded sleeper levels are small; only locations where deflections are large, possibly due to voiding, show significant differences between the two datasets.

**Table 3.** Summary statistics for sleeper deflections and support system modulus.

	Deflection (mm)			Modulus ( $\text{MN/m}^2$ )		
	Javelin	Eurostar	Velaro	Javelin	Eurostar	Velaro
Mean	0.84	1.04	1.25	27.1	23.1	24.1
Median	0.66	0.85	1.07	27.4	22.9	23.9
Mode	0.6	0.8	0.8	27	23	24
Standard deviation	0.56	0.71	0.69	10.4	9.1	7.5

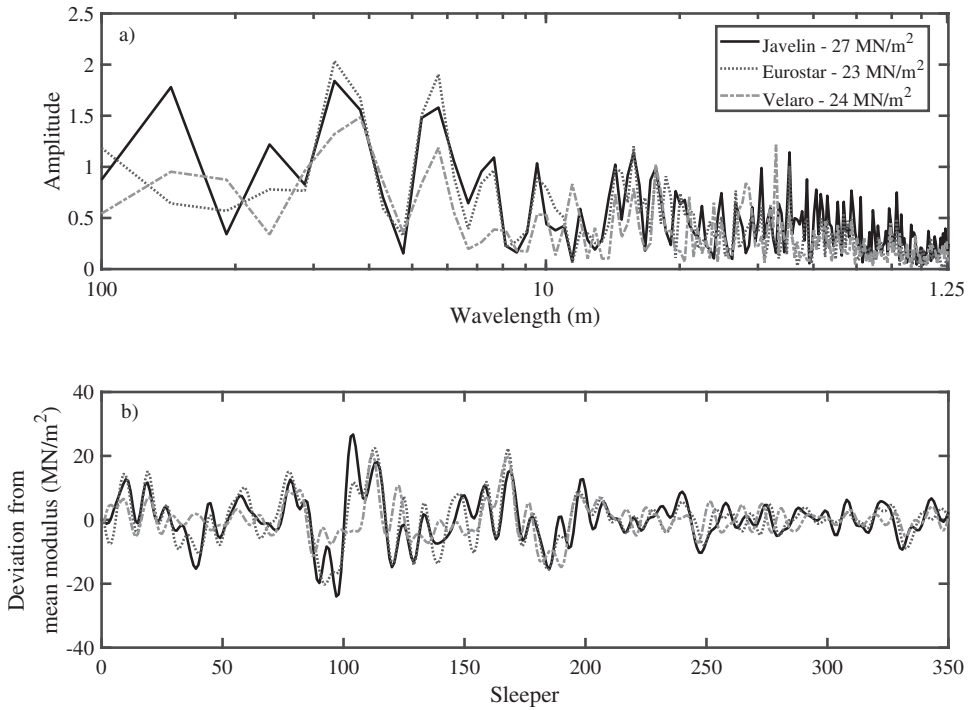


**Figure 10.** (a) Track support system modulus spectrum by wavelength, (b) Track support system modulus from Figure 8, band pass filtered between 4 and 40 m.

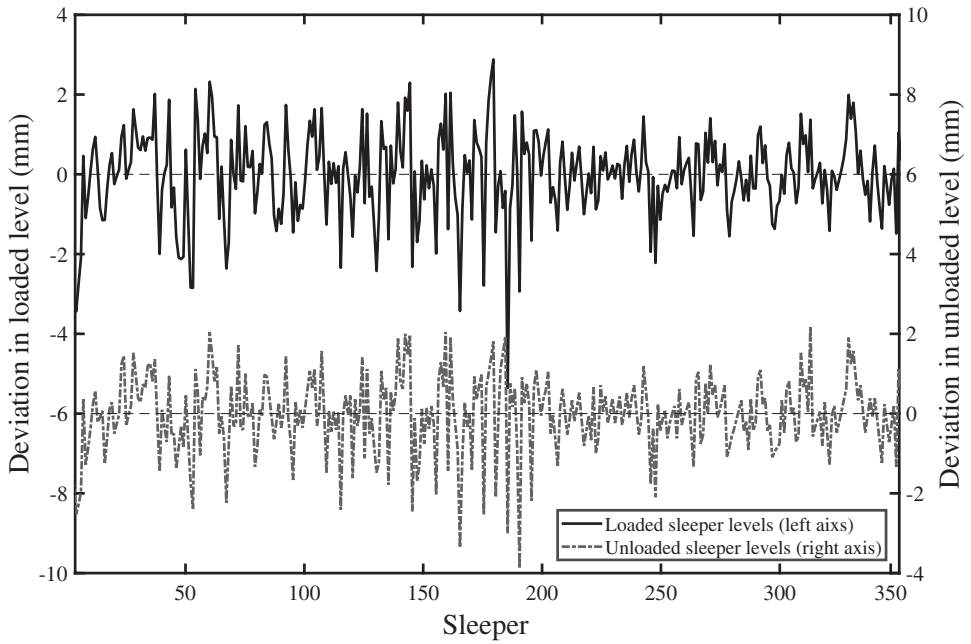


**Figure 11.** Comparison of loaded and unloaded sleeper levels.

## Simulations

All of the simulations were carried out in the time domain with a train model representative of a Class 395 Javelin. Three initial simulations (Table 4) investigated the role of track level and stiffness heterogeneity by accounting for (i) the irregularity of the rail, based on the unloaded sleeper levels, (ii) the variability in the track support system modulus and (iii) both of these. Where the track model was parameterised from measurements, the results for the Javelin were used. A fourth simulation (Table 4) was carried out to investigate the effect of possible gaps between certain sleepers and the ballast, inferred from the measurement data.

All simulations were carried out for a train speed of 60 m/s, the same as the Javelins at the measurement location. Simulations were run both with and without the 1.4% gradient, which made no difference to the results.

The initial, deformed rail geometry was determined by solving a static version of the numerical track model, in which the vertical sleeper positions were prescribed as sleeper displacements from the idealised zero level in response to a compatible set of forces acting at each sleeper. The resulting deflected shape of the rail along its whole length, (i.e. not only at the sleeper locations) was extracted and used for the simulations 1, 3, and 4.

The gaps in Simulation 4 were introduced in areas where Simulation 3 underpredicted the measured deflection by more than 0.5 mm. The gaps were sized in 0.5 mm increments according to difference between the measured and simulated results for the individual sleeper. The unseated stiffness of the ballast spring was taken as 5 kN/m, as already described. The seated stiffnesses were between 2 and 70 MN/m, based on the measurement for the individual sleeper. The locations and sizes of the gaps are given Table 5.

Downward sleeper deflections obtained from the simulations were analysed using the same frequency domain technique as used to obtain the track modulus from the original measurements. This was to test whether the input modulus values were returned, hence assess the reliability of the method of determining the support system modulus using larger datasets, with realistic variation, than previously [42,43].

Simulation 1 was designed to represent a conventional vehicle / track interaction analysis using the measured track geometry with uniform support stiffness. Figure 12(a) shows

**Table 4.** Summary of initial simulations.

Simulation	Level	Track Modulus	Voiding
1	Measured*	Uniform: 30 M/m <sup>2</sup>	None
2	Smooth	Measured <sup>†</sup>	None
3	Measured*	Measured <sup>†</sup>	None
4	Measured*	Measured <sup>†</sup>	Included

\*from total-station survey data.

<sup>†</sup>estimated from accelerometer measurements.

**Table 5.** Gap sizes for Simulation 4.

Sleeper No.	14	15	46	47	48	49	52	53	88	89	97
Void gap (mm)	1	1	1.5	2.5	2.5	1	2	2	1	1	1
Sleeper No.	98	119	130	175	183	184	185	249	278	312	336
Void gap (mm)	1	1	1	0.5	1	1.5	1	0.5	0.5	0.5	1



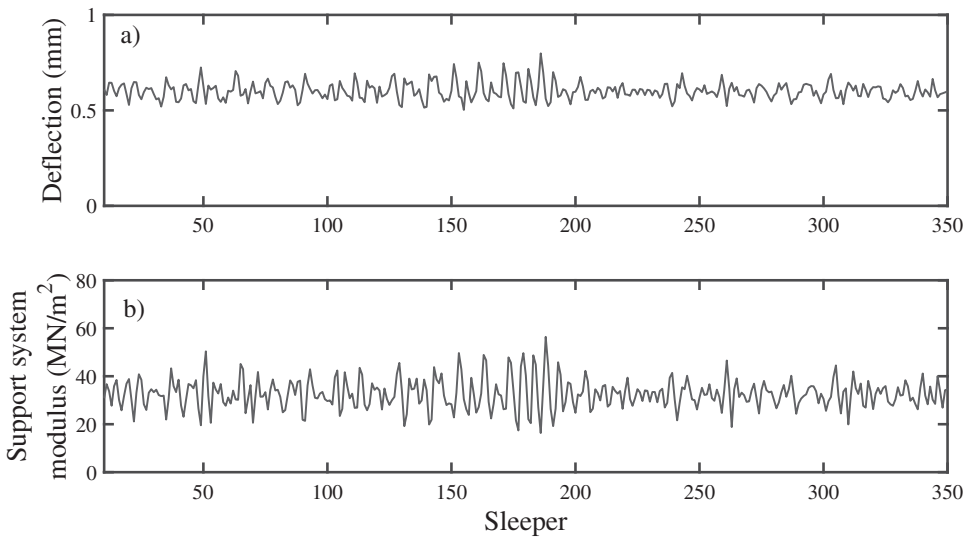


**Figure 12.** (a) Simulated downward sleeper deflections, (b) re-analysed support system modulus using measured sleeper heights on a track with a uniform support system modulus of 30 MN/m<sup>2</sup>.

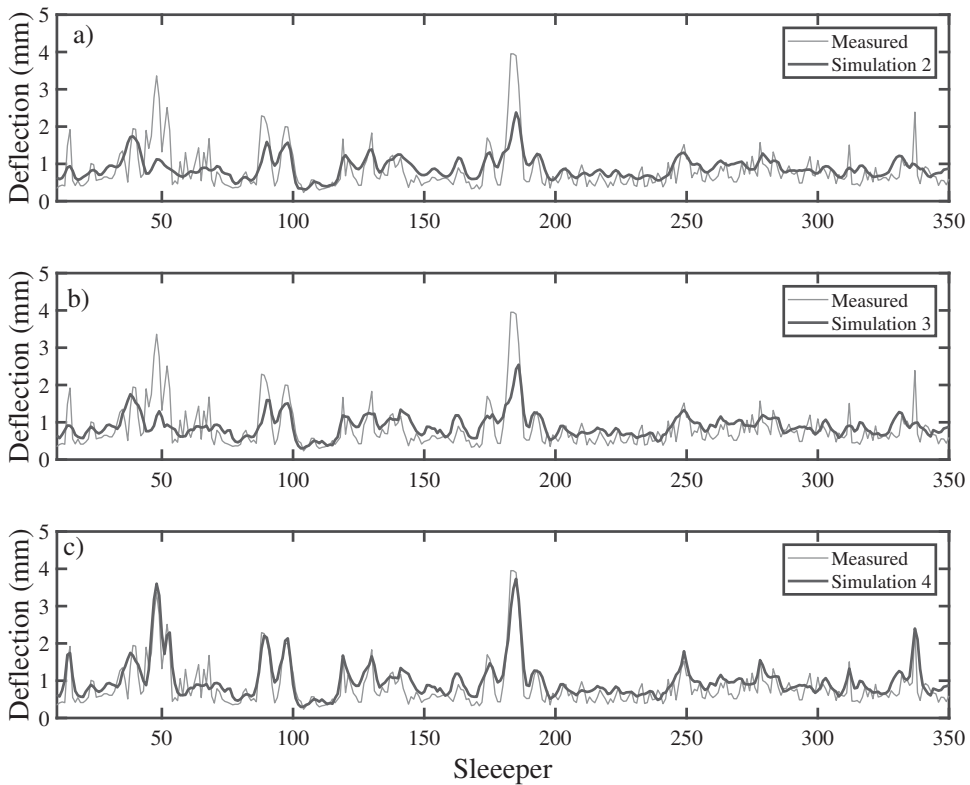
the maximum downward simulated sleeper deflections and (b) the support system moduli obtained by analysing the spectrum for the simulated sleeper displacement along the track. The simulation does not replicate the observed sleeper deflections, which remain fairly uniform at around 0.6 mm. The support system modulus returned varied around the input value of 30 MN/m<sup>2</sup>.

Figure 13 shows the downward sleeper deflections (positively signed) and Figure 14 the inferred support system moduli returned for Simulations 2, 3 and 4.

Table 6 compares summary statistics for the simulations with the measurements in Table 3, and provides the correlation and root mean square error between the measurements and the simulations.

Simulation 2 used a level track and the measured track support system stiffnesses. Figure 13 suggests that specifying the ballast springs to match the measured support system modulus resulted in a simulation that replicated the majority of measured sleeper deflections in a way that was correlated with the measurements. Including the correct relative unloaded sleeper levels did not significantly affect the calculated sleeper deflections. Introducing gaps between the sleepers and the ballast in locations where Simulation 3 underpredicted the sleeper deflections (whose locations and magnitudes were given in Table 5) improved the correlation and reduced the root mean square error between the simulated and measured deflections.

In all cases the simulated deflections were minimally larger than the measurements; in Figure 13, the simulations never reach the deflection floor of the measurements and they were less variable than the measurements. These differences may be due out of plane effects such as differences in cross-level and / or support stiffness at each end of a sleeper. This was not studied, nor can it be simulated in a two-dimensional model. Alternatively, it is possible that the static stiffnesses specified were too low, owing to train speed effects influencing the measurement.



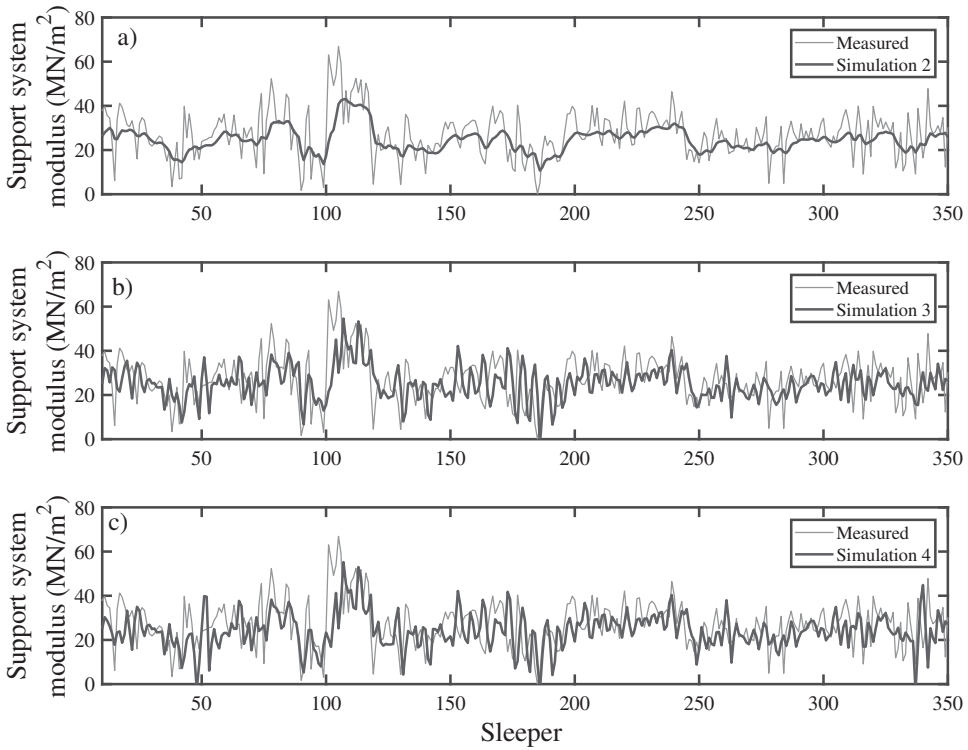
**Figure 13.** Measured and Simulated downward sleeper deflections for 350 sleepers, including progressively (a) variable support conditions, (b) sleeper heights and (c) voiding.

Figure 14 shows the support system moduli returned from the simulation using the same frequency-based analysis as for the lineside measurements. The average stiffness was around 24–25 MN/m<sup>2</sup>, minimally less than the measured results. For smooth track (Simulation 1), the results were correlated with the measurements but were less variable (lower standard deviation), with better correlation from sleeper to sleeper than in the measurements. The track system appears to smooth out the heterogeneity in support stiffness specified on the basis of the measurements. Including the unloaded sleeper levels and voids in the simulation led to a reduced correlation with the measured modulus and increased the root mean square error, owing to an increase in the general level of disagreement overall. However, the central values for modulus were unchanged, and the standard deviation increased such that the variability of the irregular and voided simulation was closest to that of the measurements.

### **Contact forces and wheel position**

The results of the simulations may also be used to investigate vehicle behaviour. Figure 15 shows the calculated wheel-rail contact forces and Figure 16 the calculated wheel position for the leading wheel of the train.

Figure 15 shows that the results for the simulations starting from the measured unloaded sleeper levels were all similar, regardless of the support conditions, and were different from



**Figure 14.** Measured and Simulated inferred support sleeper moduli for 350 sleepers, including progressively (a) variable support conditions, (b) sleeper heights and (c) voiding.

**Table 6.** Summary statistics for the simulations with Javelin train using measured support stiffnesses.

	Downward deflection (mm)				Modulus (MN/m <sup>2</sup> )			
	Measured	Simulation 2	Simulation 3	Simulation 4	Measured	Simulation 2	Simulation 3	Simulation 4
Mean	0.84	0.88	0.89	0.99	27.1	24.5	25.2	24.3
Median	0.66	0.84	0.86	0.87	27.3	24.3	25.0	24.5
Mode	0.6	0.7	0.9	0.7	27	24	25	24
Standard deviation	0.56	0.28	0.29	0.50	10.3	5.2	7.5	8.2
Correlation with measurement (%)	–	68	66	85	–	70	55	46
Root mean square error	–	0.42	0.44	0.33	–	2.5	2.9	3.2

and more variable than the result for a smooth rail with variable support conditions. The mean contact force was 55.4 kN (the static wheel load) in all simulations. However, the standard deviation was about 5 kN (9%) for all of the irregular rail level cases (Simulations 1, 3 and 4), but only about 1.1 kN (2%) for the smooth track with variable support (Simulation 2). The root mean squares of the differences between the results with an irregular level were all less than 3.5 kN (6%). In these simulations, variations in the unloaded track level caused more significant differences in wheel / rail contact forces than variations in support stiffness.

The support system moduli found from the simulations (Figure 14) showed that it was necessary to include the irregular unloaded track level and under-sleeper voiding to repro-

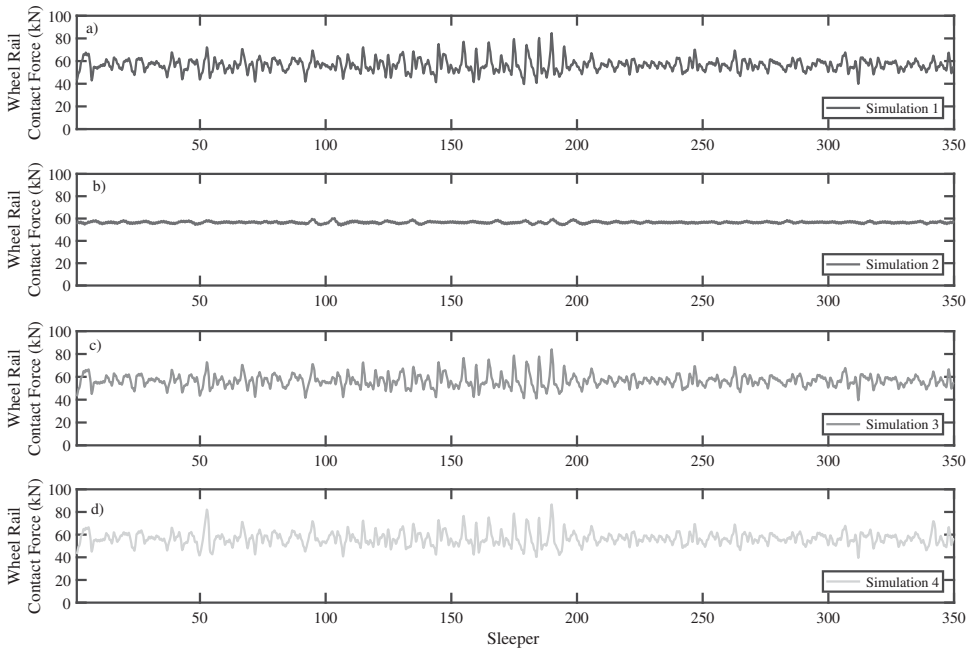


**Figure 15.** Simulated wheel / rail contact force.

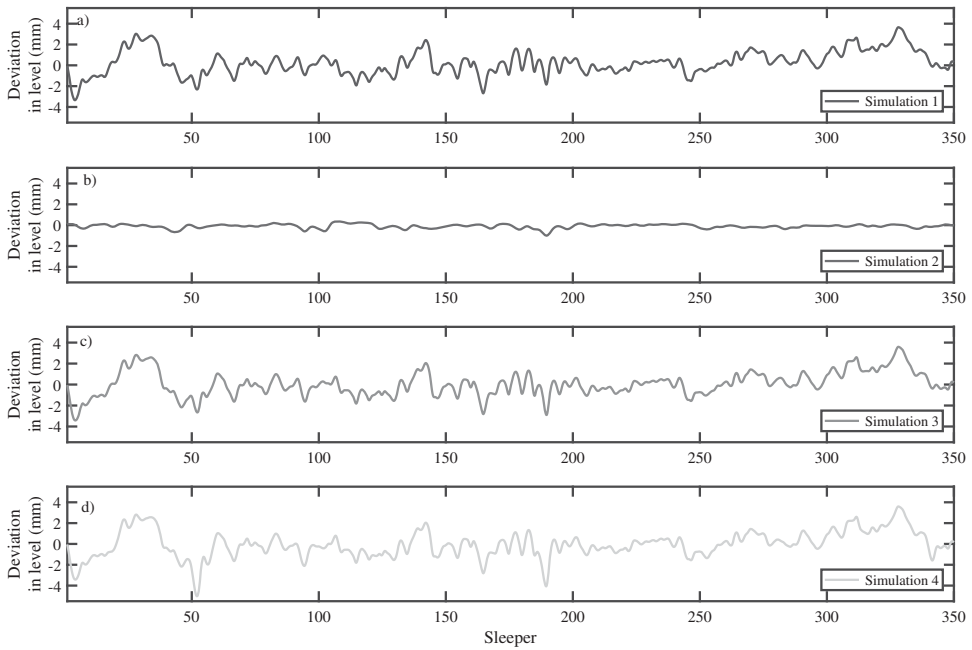


**Figure 16.** Simulated wheel displacement for different track conditions.

duce the measured variability. Figure 15 shows that the unloaded track level is important for the variation in wheel / rail contact force, which may at least partly explain why reproducing the variability seen in the measured support system modulus data required the input of accurate unloaded rail level data.

Figure 16 shows that simulating the measured variation in support system stiffness does not lead to as significant a difference in the wheel position as variations in the unloaded sleeper levels and any under-sleeper gaps.

Together, these measurements and simulations suggest that for the ranges typified by this section of track the unloaded level of the track is more significant for the prediction of wheel / rail contact forces than the differential deflection arising from variable support conditions. Conversely, the variations in the track support system stiffness are important for calculating realistic track deflections and, by implication (but not studied here), the trackbed forces and stresses in the ground that are likely to be relevant for the prediction of permanent settlement. The inertia of the track may also play a role. These findings are consistent with recent work by [47] using rolling stiffness and geometry measurements over a long length of track.

The findings have implications for monitoring and simulation to inform long term management of track performance, particularly over extended lengths of track. Simulation of vehicle track interaction could be de-coupled from modelling of the track when calculating the contact forces, which could then be input into a track model whose response could be

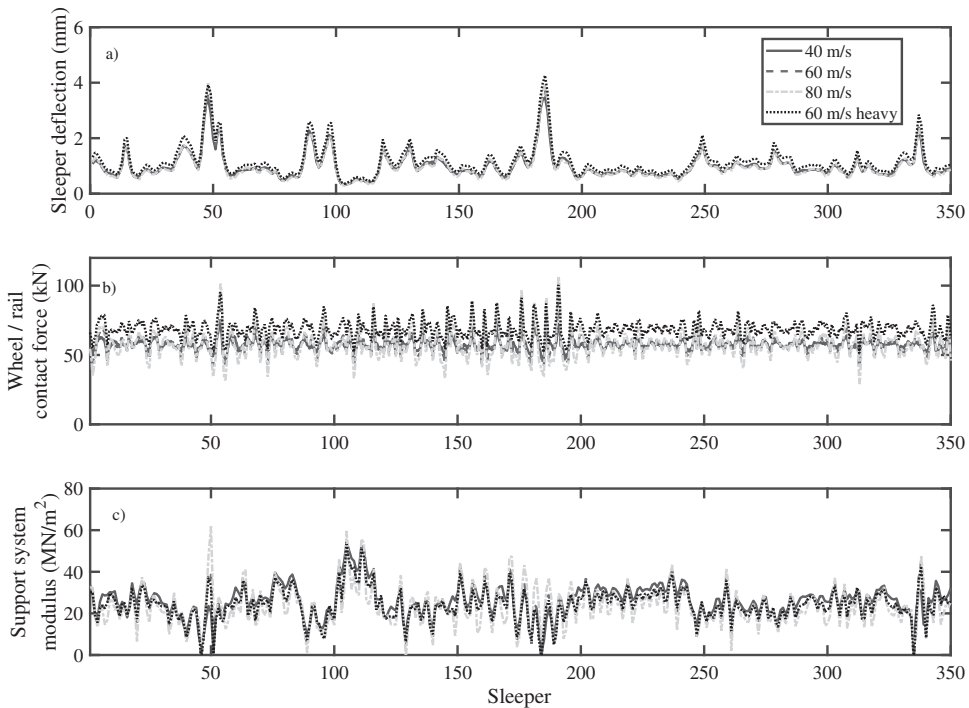


**Figure 17.** (a) Simulated downward sleeper deflections and (b) re-analysed support system modulus for different train speeds and increased carbody mass; irregular and voided track with variable support stiffness.

used to forecast changes in track level using a more realistic model for subgrade / trackbed deterioration; i.e. separate and possibly simpler models could be used.

### *Speed and load*

Figures 7 and 8 indicated differences between the behaviour of the track under a Javelin train and that under a Eurostar or a Velaro, both of which operate at a higher speed and are heavier than the Javelin. To investigate the influence of speed and load, further simulations were carried out using the irregular and voided track with variable sleeper support, and the Javelin type vehicle. Train speeds of 40, 60 and 80 m/s were simulated and the 60 m/s simulation was repeated with a 25% increase in car body mass. The results of these simulations are shown in Figure 17.

Figure 17(a) shows that the train speed did not have any significant effect on the calculated sleeper deflections, whereas increasing the car body mass (and thereby the wheel load) resulted in an increase in sleeper deflections. In these simulations, speed would only be expected to cause an increase in deflection if the track were sufficiently irregular to create large impact loads, or if the train speed were to approach the critical velocity of the track / support system [60]. The speed does increase the peak wheel-rail contact forces, Figure 17(b). In Figure 17(c) increasing the speed reduced the mean values of track system support stiffness returned from 26.1 MN/m<sup>2</sup> to 24.3 MN/m<sup>2</sup> to 23.3 MN/m<sup>2</sup> for 40, 60 and 80 m/s respectively. As with the apparent softening seen in Figure 8 for the faster trains, this reduction may be due to analysing a dynamic simulation using a static definition of track system support modulus.

### **Conclusions**

Track support system moduli, unloaded track geometry and sleeper deflections under load have been measured during the passage of  $\sim 40$  trains, at successive sleepers over a 200 m length of track. The measurements showed a degree of variation from sleeper to sleeper, and were used to parameterise simulations carried out using a vehicle track interaction model, with varying degrees of sophistication in terms of modelling the real variations in unloaded track level, track support system modulus from sleeper to sleeper, and the presence of voids below individual sleepers. On the basis of the measurements and simulations, for the ranges of stiffness and initial level variation and voiding measured:

- Differences in unloaded sleeper levels had more of an influence on the loaded level of the track than variations between individual sleeper deflections under load.
- The unloaded track level had more of an influence on calculated wheel / rail contact forces than varying the sleeper support stiffness.
- The measured sleeper deflections were reproduced more closely in simulations in which the measured variation in support system modulus from sleeper to sleeper was taken into account. To reproduce the larger deflections measured, it was necessary to introduce non-linearity to represent voids below the affected sleepers.
- Analysing the simulated sleeper displacements in the same way as was used to find the track support system modulus from the measurements returned results that were similar to the input measurements. Suggesting the assumptions made for this analysis are

reasonable and practical. To reproduce realistic variability it was also necessary to use the measured unloaded sleeper levels in the simulation.

This suggests that the variation track level is significant for the vehicle dynamics and loading, while the variation in stiffness (non-linear support) is significant for the behaviour of the track. A possible implication of this is that contact forces calculated from track level could be used as an input for a track model with realistic stiffness variation. This may enable forecasts of realistic performance along longer lengths of track using separate, simpler models rather than simulating track and vehicle together in a single, more complex model.

## Acknowledgements

The research was funded by the Engineering and Physical Sciences Research Council (EPSRC) through the programme grant Track to the Future (EP/M025276/1). This work would also not have been possible without the kind assistance given by Mick Hayward and Sin Sin Hsu of Network Rail High Speed and support of Geoff Watson, Tristan Rees-White, Taufan Abadi and Ali Shabaz-Kahn from the University of Southampton. The Authors declare that there are no conflicts of interest. Data and supplementary details supporting this study are openly available from the University of Southampton repository at <https://doi.org/10.5258/SOTON/D1095>.

## Disclosure statement

No potential conflict of interest was reported by the authors.

## Funding

This work was supported by Engineering and Physical Sciences Research Council [Grant Number EP/M025276/1].

## ORCID

David Milne  <http://orcid.org/0000-0001-6702-3918>

John Harkness  <http://orcid.org/0000-0001-7598-0080>

Louis Le Pen  <http://orcid.org/0000-0002-4362-3895>

William Powrie  <http://orcid.org/0000-0002-2271-0826>

## References

- [1] Digital Railway. Digital[Q4] railway strategy. London: Network Rail; 2018.
- [2] British Standards Institution. BS EN 13848. Railway applications - Track - Track geometry quality. London.
- [3] Jenkins HH, Stephenson JE, Clayton GA. Effect of track and vehicle parameters on wheel/rail vertical dynamic forces. *Railw Eng J*. 1974;3(2):2–16.
- [4] Timoshenko S, Langer BF. Stresses in railroad track. *ASME Trans*. 1932;54:277–293.
- [5] Resonate Group Ltd. Vampire Dynamics; 2016.
- [6] Transportation Technology Centre Inc. NUCARS; 2016.
- [7] VI-Grade. VI-Rail; 2016.
- [8] Iwnicki S. Handbook of railway vehicle dynamics. London: CRC Press; 2006.
- [9] Fröhling RD. Low frequency dynamic vehicle/track interaction: modelling and simulation. *Veh Syst Dyn*. 1998 Jan;29(1):30–46. doi:10.1080/00423119808969550.



- [10] Grossoni I, Andrade AR, Bezin Y, et al. The role of track stiffness and its spatial variability on long-term track quality deterioration. *Proc Inst Mech Eng, Part F: J Rail Rapid Transit.* 2019;233(1):16–32. doi:10.1177/0954409718777372.
- [11] Nielsen JCO, Igeland A. Vertical dynamic interaction between train and track influence of wheel and track imperfections. *J Sound Vib.* 1995 Nov;187(5):825–839. doi:10.1006/jsvi.1995.0566.
- [12] Shih JY, Thompson DJ, Zervos A. The influence of soil nonlinear properties on the track/ground vibration induced by trains running on soft ground. *Transp Geotech.* 2017 Jun;11:1–16. doi:10.1016/j.trgeo.2017.03.001.
- [13] Varandas JN, Hölscher P, Silva MAG. Three-dimensional track-ballast interaction model for the study of a culvert transition. *Soil Dyn Earthq Eng.* 2016 Oct;89:116–127. doi:10.1016/j.soildyn.2016.07.013.
- [14] Ferreira PA, Lopez-Pita A. Numerical modeling of high-speed train/track system to assess track vibrations and settlement prediction. *J Trans Eng-Asce.* 2013;139(3):330–337. doi:10.1061/(asce)te.1943-5436.0000482.
- [15] Grassie SL, Gregory RW, Harrison D, et al. The dynamic response of railway track to high frequency vertical excitation. *J Mech Eng Sci.* 1982 Jun;24(2):77–90. doi:10.1243/jmes\_jour\_1982\_024\_016\_02.
- [16] Yang LA, Powrie W, Priest JA. Dynamic stress analysis of a ballasted railway track bed during train passage. *J Geotech Geoenviron Eng.* 2009;135(5):680–689. doi:10.1061/(ASCE)GT.1943-5606.0000032.
- [17] Zhai W, Cai Z. Dynamic interaction between a lumped mass vehicle and a discretely supported continuous rail track. *Comput Struct.* 1997 Jun;63(5):987–997. doi:10.1016/S0045-7949(96)00401-4.
- [18] Dahlberg T. Railway track stiffness variations—consequences and countermeasures. *Int J Civ Eng.* 2010;8(1):1–11.
- [19] Track Stiffness Working Group. A guide to track stiffness. Southampton: University of Southampton; 2016. (Powrie W, Le Pen L, editors.).
- [20] Cui Y-J, Lamas-Lopez F, Trinh VN, et al. Investigation of interlayer soil behaviour by field monitoring. *Transp Geotech.* 2014 Sep;1(3):91–105. doi:10.1016/j.trgeo.2014.04.002.
- [21] Le Pen L, Watson G, Powrie W, et al. The behaviour of railway level crossings: Insights through field monitoring. *Transp Geotech.* 2014;1(4):201–213. doi:10.1016/j.trgeo.2014.05.002.
- [22] Mishra D, Qian Y, Huang H, et al. An integrated approach to dynamic analysis of rail-road track transitions behavior. *Transp Geotech.* 2014 Dec;1(4):188–200. doi:10.1016/j.trgeo.2014.07.001.
- [23] Paixão A, Fortunato E, Calçada R. Transition zones to railway bridges: track measurements and numerical modelling. *Eng Struct.* 2014 Dec;80:435–443. doi:10.1016/j.engstruct.2014.09.024.
- [24] Wheeler LN, Take WA, Hoult NA. Measurement of rail deflection on soft subgrades using DIC. *Proc Inst Civ Eng - Geotech Eng.* 2016;169(5):383–398. doi:10.1680/jgeen.15.00171.
- [25] Berggren EG, Nissen A, Paulsson BS. Track deflection and stiffness measurements from a track recording car. *Proc Inst Mech Eng, Part F: J Rail Rapid Transit.* 2014 Aug;228(6):570–580. doi:10.1177/0954409714529267.
- [26] Fallah Nafari S, Gül M, Roghani A, et al. Evaluating the potential of a rolling deflection measurement system to estimate track modulus. *Proc Inst Mech Eng, Part F: J Rail Rapid Transit.* 2018 Jan;232(1):14–24. doi:10.1177/0954409716646404.
- [27] Oscarsson J. Dynamic train-track interaction: variability attributable to scatter in the track properties. *Veh Syst Dyn.* 2002 Jan;37(1):59–79. doi:10.1076/vesd.37.1.59.3538.
- [28] Oscarsson J. Simulation of train-track interaction with stochastic track properties. *Veh Syst Dyn.* 2002 Jun;37(6):449–469. doi:10.1076/vesd.37.6.449.3521.
- [29] Li MXD, Berggren EG. A study of the effect of global track stiffness and its variations on track performance: Simulation and measurement. *Proc Inst Mech Eng, Part F: J Rail Rapid Transit.* 2010;224(5):375–382. doi:10.1243/09544097jrtr361.

- [30] Milne D, Le Pen L, Watson G, et al. Monitoring and repair of isolated trackbed defects on a ballasted railway. *Transp Geotech.* 2018 Dec;17:61–68. doi:10.1016/j.trgeo.2018.09.002.
- [31] Wang H, Markine V. Modelling of the long-term behaviour of transition zones: prediction of track settlement. *Eng Struct.* 2018 Feb;156:294–304. doi:10.1016/j.engstruct.2017.11.038.
- [32] Li D, Davis D. Transition of Railroad Bridge Approaches. *J Geotech Geoenviron Eng.* 2005;131(11):1392–1398. doi:10.1061/(ASCE)1090-0241(2005)131:11(1392).
- [33] Lamas-Lopez F, Cui Y-J, Calon N, et al. Track-bed mechanical behaviour under the impact of train at different speeds. *Soils Found.* 2016 Sep;56(4):627–639. doi:10.1016/j.sandf.2016.07.004.
- [34] Powrie W, Yang LA, Clayton CRI. Stress changes in the ground below ballasted railway track during train passage. *Proc Inst Mech Eng, Part F: J Rail Rapid Transit.* 2007 Mar;221(2):247–262. doi:10.1243/0954409jrtr95.
- [35] Priest JA, Powrie W, Yang LA, et al. Measurements of transient ground movements below a ballasted railway line. *Géotechnique.* 2010;60:667–677. En.
- [36] Sadri M, Steenbergen M. Effects of railway track design on the expected degradation: Parametric study on energy dissipation. *J Sound Vib.* 2018 Apr;419:281–301. doi:10.1016/j.jsv.2018.01.029.
- [37] Bowness D, Lock AC, Powrie W, et al. Monitoring the dynamic displacements of railway track. *Proc Inst Mech Eng, Part F: J Rail Rapid Transit.* 2007;221(1):13–22. doi:10.1243/0954409jrtr51.
- [38] Kerr AD. On the determination of the rail support modulus k. *Int J Solids Struct.* 2000 Aug;37(32):4335–4351. doi:10.1016/S0020-7683(99)00151-1.
- [39] Priest J, Powrie W. Determination of dynamic track modulus from measurement of track velocity during train passage. *J Geotech Geoenviron Eng.* 2009;135(11):1732–1740. doi:10.1061/(ASCE)GT.1943-5606.0000130.
- [40] Raymond GP. Analysis of track support and determination of track modulus. *Transp Res Rec.* 1985;1022:80–90.
- [41] Wheeler LN, Take WA, Hoult NA. Performance assessment of peat rail subgrade before and after mass stabilization. *Can Geotech J.* 2017 May;54(5):674–689. doi:10.1139/cgj-2016-0256.
- [42] Le Pen L, Milne D, Thompson D, et al. Evaluating railway track support stiffness from track-side measurements in the absence of wheel load data. *Can Geotech J.* 2016;53(7):1156–1166. doi:10.1139/cgj-2015-0268.
- [43] Milne D, Le Pen LM, Thompson DJ, et al. Properties of train load frequencies and their applications. *J Sound Vib.* 2017 Jun;397:123–140. doi:10.1016/j.jsv.2017.03.006.
- [44] Coelho B, Hölscher P, Priest J, et al. An assessment of transition zone performance. *Proc Inst Mech Eng, Part F: J Rail Rapid Transit.* 2011 Mar;225(2):129–139. doi:10.1177/09544097jrtr389.
- [45] Le Pen L, Watson G, Hudson A, et al. Behaviour of under sleeper pads at switches and crossings – Field measurements. *Proc Inst Mech Eng, Part F: J Rail Rapid Transit.* 2018 Apr;232(4):1049–1063. doi:10.1177/0954409717707400.
- [46] Stark TD, Wilk ST. Root cause of differential movement at bridge transition zones. *Proc Inst Mech Eng, Part F: J Rail Rapid Transit.* 2015 Jun. doi:10.1177/0954409715589620.
- [47] Germonpré M, Nielsen JCO, Degrande G, et al. Contributions of longitudinal track unevenness and track stiffness variation to railway induced vibration. *J Sound Vib.* 2018 Dec;437:292–307. doi:10.1016/j.jsv.2018.08.060.
- [48] Onshore Borehole scans [Internet]. British Geological Survey (NERC). 1999 [cited 2017].
- [49] Milne D, Le Pen L, Watson G, et al. Proving MEMS technologies for smarter railway infrastructure. *Procedia Eng.* 2016;143:1077–1084. doi:10.1016/j.proeng.2016.06.222.
- [50] Milne D, Le Pen L, Thompson DJ, et al. Automated processing of railway track deflection signals obtained from velocity and acceleration measurements. *Proc Inst Mech Eng, Part F: J Rail Rapid Transit.* 2018;232(8):2097–2110. doi:10.1177/0954409718762172.

- [51] Kerr AD. On the determination of foundation model parameters. *J Geotechn Eng.* 1985;111(11):1334–1340. doi:10.1061/(ASCE)0733-9410(1985)111:11(1334).
- [52] Auersch L. Ground vibration due to railway traffic—The calculation of the effects of moving static loads and their experimental verification. *J Sound Vib.* 2006 Jun;293(3–5):599–610. doi:10.1016/j.jsv.2005.08.059.
- [53] Ju S-H, Lin H-T, Huang J-Y. Dominant frequencies of train-induced vibrations. *J Sound Vib.* 2009 Jan;319(1–2):247–259. doi:10.1016/j.jsv.2008.05.029.
- [54] Ferrara R, Leonardi G, Jourdan F. Numerical modelling of train induced vibrations. *Procedia - Social Behav Sci.* 2012 Sep;53:155–165. doi:10.1016/j.sbspro.2012.09.869.
- [55] Sun YQ, Dhanasekar M. A dynamic model for the vertical interaction of the rail track and wagon system. *Int J Solids Struct.* 2002 Mar;39(5):1337–1359. doi:10.1016/S0020-7683(01)00224-4.
- [56] Zhai W, Sun X. A detailed model for investigating vertical interaction between railway vehicle and track. *Veh Syst Dyn.* 1994 Jan;23(sup1):603–615. doi:10.1080/00423119308969544.
- [57] Knothe KL, Grassie SL. Modelling of railway track and vehicle/track interaction at high frequencies. *Veh Syst Dyn.* 1993 Jan;22(3–4):209–262. doi:10.1080/00423119308969027.
- [58] Sussman T, Ebersöhn W, Selig E. Fundamental Nonlinear track load-deflection Behavior for Condition evaluation. *Transp Res Rec: J Transp Res Board.* 2001;1742:61–67. doi:10.3141/1742-08.
- [59] Wheeler LN, Take WA, Hoult NA, et al. The Use of Fiber Optic Sensing to measure distributed rail Strains and Determine rail Seat forces Due to a Moving train. *Can Geotech J.* 2018. doi:10.1139/cgj-2017-0163.
- [60] Thompson D. *Railway noise and vibration mechanisms, modelling and means of control.* Oxford: Elsevier; 2009.
- [61] Zhai WM, Wang KY, Lin JH. Modelling and experiment of railway ballast vibrations. *J Sound Vib.* 2004 Mar;270(4):673–683. doi:10.1016/S0022-460X(03)00186-X.
- [62] Li Q, Thompson DJ, Toward MGR. Estimation of track parameters and wheel-rail combined roughness from rail vibration. *Proc Inst Mech Eng, Part F: J Rail Rapid Transit.* 2018 Apr;232(4):1149–1167. doi:10.1177/0954409717710126.
- [63] Abadi T. *Effect of sleeper and ballast interventions on rail track performance.* University of Southampton; 2015.
- [64] Pita AL, Teixeira PF, Robuste F. High speed and track deterioration: The role of vertical stiffness of the track. *Proc Inst Mech Eng, Part F: J Rail Rapid Transit.* 2004 Jan;218(1):31–40. doi:10.1243/095440904322804411.
- [65] Rail Safety and Standards Board. *GC/RT5021 track system requirements.* London: RSSB; 2011.
- [66] Selig ET, Li D. Track modulus: Its meaning and factors influencing it. *Transp Res Rec.* 1994;1470:47–54.